ADVANCED FUNCTIONAL MATERIALS
www.afm-journal.de

Growth and Transfer of Monolithic Horizontal ZnO Nanowire Superstructures onto Flexible Substrates

By *Sheng Xu, Yue Shen, Yong Ding,* and *Zhong Lin Wang**

A method of fabricating horizontally aligned ZnO nanowire (NW) arrays with full control over the width and length is demonstrated. A cross-sectional view of the NWs by transmission electron microscopy shows a "mushroom-like" structure. Novel monolithic multisegment superstructures are fabricated by making use of the lateral overgrowth. Ultralong horizontal ZnO NWs of an aspect ratio on the order of ten thousand are also demonstrated. These horizontal NWs are lifted off and transferred onto a flexible polymer substrate, which may have many great applications in horizontal ZnO NW-based nanosensor arrays, light-emitting diodes, optical gratings, integrated circuit interconnects, and high-output-power alternating-current nanogenerators.

1. Introduction

ZnO is a piezoelectric material with a wide direct bandgap of 3.37 eV and a large exciton binding energy of 60 meV.[1] It has been demonstrated to have enormous applications in building up electronic, optoelectronic, electrochemical, and electromechanical nanodevices, such as UV lasers,[2] light-emitting diodes,[3,4] field-emission devices,[5] solar cells,[6] high-performance nanosensors,[7] piezoelectric nanogenerators,[8] and nano-piezotronics.[9] ZnO nanowires (NWs) have been synthesized by a wide range of approaches, such as physical vapor deposition,[10] wet chemical methods,[11] pulsed laser deposition,[12] metal–organic chemical vapor deposition,[13] molecular beam epitaxy,[14] and so on. By controlling the synthesis parameters, control has been demonstrated over their morphology, dimensionality, and aspect ratio, which were usually easily entangled with each other. In order to integrate the ZnO NWs into functional nanodevices, Vayssieres et. al developed vertically aligned ZnO NW arrays by coating a substrate prior to the wet chemical growth with a ZnO seed thin film,[15] which was polycrystalline and thus the vertical alignment of the arrays was rather poor. By employing an epitaxial growth relationship on single-crystalline substrates, almost perfectly vertically aligned arrays were grown on GaN,[16] AlN,[17] SiC,[18] Al_2O_3,[19] and $MgAl_2O_4$[20] substrates. In an effort to arrange the NWs into a more regular form to further enhance the performance of the nanodevices, the positions of the NWs on the substrate could be controlled by a variety of techniques, including photolithography,[21] nanosphere lithography,[22] nanoimprint lithography,[23] and electron-beam lithography.[24]

As a counterpart to vertical arrays, horizontal arrays have their own uniqueness and may have as many potential applications as the vertical ones, but there is only limited research and progress in this area. For instance, instead of being coated on the substrate's top surface, a ZnO seed thin film was coated on the trench sidewalls on the substrate[25] so that the NWs were able to grow parallel to the substrate surface. However, the NWs were sparse and poor in horizontal alignment, and the vertical components were always not completely eliminated. Horizontal arrays were also made by controlling the surface texture of the as-deposited polycrystalline seed film with pulsed laser deposition.[26] There was a report on the epitaxial growth on an *a*-plane sapphire substrate by physical vapor deposition,[27] but the uniformity and spatial control of the NWs were rather poor. Horizontal alignment of ZnO NWs after growth was also demonstrated by dispersing the NWs in a solvent and then applying a high-frequency alternating electrical field.[28]

In our previous contribution, we showed a technique for patterned growth of horizontally aligned ZnO NW arrays by a combination of wet chemical method and electron-beam lithography.[29] The NWs were epitaxially grown on the $(2\bar{1}\,\bar{1}0)$ surface of a single-crystalline ZnO substrate with a precisely controlled orientation and distribution. Here we demonstrate the growth of horizontal ZnO NW arrays with full control over their width and length. In addition, by innovatively designing the layout of the photoresist openings (POs) on the substrate, monolithic multisegment superstructures were fabricated by virtue of lateral overgrowth of the NWs. Furthermore, by encapsulating the NW arrays with a polymer thin film, the horizontal NW arrays were lifted off and transferred onto flexible substrates, which shows great promise for many applications based on horizontal ZnO NWs, including chemical and biological nanosensors,[30,31]

[*] Prof. Z. L. Wang, S. Xu,[+] Y. Shen,[+] Dr. Y. Ding
School of Materials Science and Engineering
Georgia Institute of Technology
771 Ferst Drive, Atlanta, GA 30332 (USA)
E-mail: zlwang@gatech.edu
Y. Shen
Department of Advanced Materials and Nanotechnology
College of Engineering, Peking University
Beijing 100871 (China)
[+] These authors contributed equally to this work.

DOI: 10.1002/adfm.201000230

© 2010 WILEY-VCH Verlag GmbH & Co. KGaA, Weinheim

light-emitting diodes,[32] optical gratings,[33] integrated circuit interconnects, and high-output-power alternating-current nanogenerators.[34]

2. Results and Discussion

The reactions taking place in aqueous systems are usually considered to be in a reversible equilibrium, and the driving force is to minimize the free energy of the entire reaction system, which is the nature of wet chemical method. For wurtzite-structured ZnO NWs, along the *c*-axis they have intrinsic high-energy polar surfaces such as ±(0001).[35] Owing to the high energy of the polar surfaces, the incoming molecules tend to be favorably adsorbed on the polar surfaces and acquire energy benefits from satisfying the dangling bonds, resulting in a fast growth along ±⟨0001⟩ and the formation of low-energy, nonpolar $\{1\bar{1}00\}$ or $\{2\bar{1}\bar{1}0\}$ surfaces. This is how a NW structure is formed. In the physical vapor deposition, the width of the NW is, in a lot of cases, dictated by the size of the catalyst particle and normally doesn't change with growth time, simply because the incoming molecular species are preferably adsorbed on the catalyst particle and the growth occurs at the interface between the particle and the solid NW.[36] But in the wet chemical method, size expansion is always observed in both the vertical and horizontal directions when the NWs are grown on photoresist prepatterned substrates,[24,29,37] which is reasonable as discussed in the following. When out of the POs, the NWs experience no physical confinement and could grow along both polar and nonpolar axes, however with different growth rates due to the different adsorption rates and the slow diffusion of the precursor molecules at low temperatures. As shown in Figure 1, out of 400-nm-wide and 5-μm-long POs, the as-grown NWs are 1-μm-wide and 13.2-μm-long. The overgrowths in width and length are about 600 nm and 8.2 μm, respectively. Nevertheless, as shown in Figure 2a–d, we could still control the width and length of the NWs effectively and efficiently by defining different sizes of the POs.[24,29] We can clearly see that the size of the NWs increases with enlarging the size of the POs, but they are apparently not in a linear relationship.

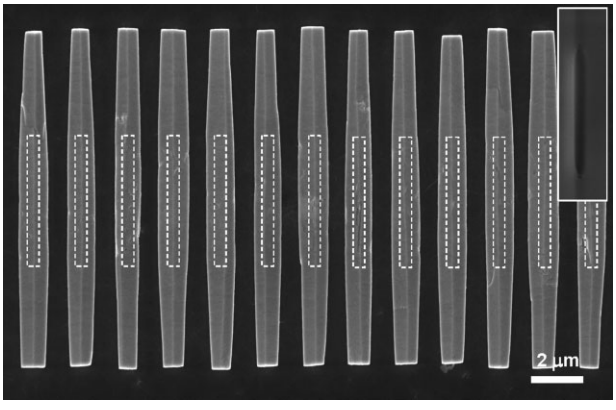

Figure 1. Lateral expansion of the horizontal NW arrays. The white dashed lines indicate the actual size of the POs out of which the NWs grew. Inset image on the upper right corner (at the same magnification) is the real SEM image of the PO.

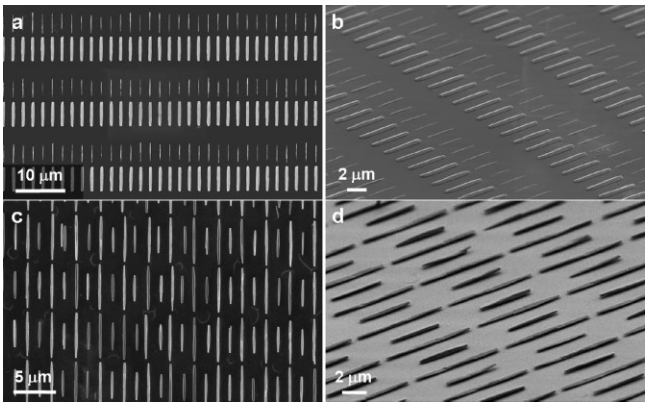

Figure 2. SEM images of horizontal ZnO NWs of different widths and lengths. a) Top view and b) 30° tilted view of the thick (~550-nm-wide out of 200-nm-wide POs) and thin NWs (~100-nm-wide out of 50-nm-wide POs). c) Top view and d) 30° tilted view of the long (~7.5 μm in length out of 4-μm POs) and short NWs (~4.5 μm in length out of 1-μm POs).

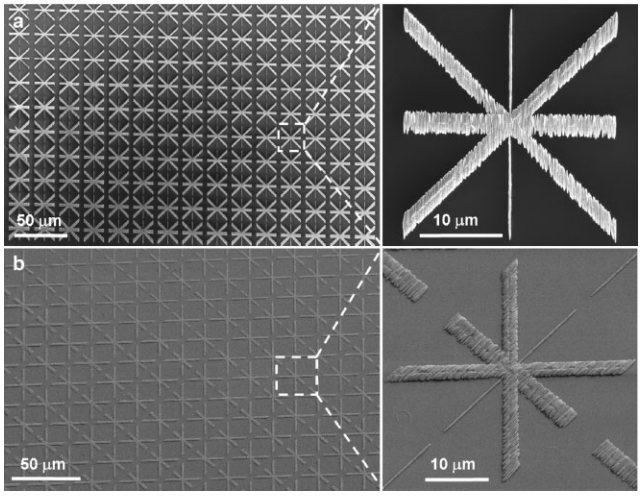

Figure 3. Illustration of the relationship between the ZnO NW growth direction and the PO orientation on the substrate. a) Top overhead view and b) 30° tilted view of the horizontal ZnO NW arrays growing out of an array of cross marks.

The substrate, an *a*-plane $(2\bar{1}\bar{1}0)$ single-crystalline ZnO wafer, has the *c*-axis lying inside the top surface plane, so we have to be careful about the orientation of the POs, parallel or perpendicular to the *c*-axis. Because the NWs always grow along the *c*-axis, for these POs parallel to the *c*-axis, one opening gives rise to one NW. For these not parallel to the *c*-axis, each and every single point along the openings could be considered as a seed and give rise to one NW with approximately the same growth rates along both the *c*- and –*c*-directions.[29] These NWs pile up side by side together, forming a ZnO NW slab (Fig. 3). The precursor concentration plays an important role here.[38] What we normally used is 5 mM, but when it goes to a relatively low level (1 mM), these side-by-side NWs will not merge with each other (see Supporting Information, Fig. S1). Instead of making strips, we can also make dotted patterns on the

WILEY InterScience DISCOVER SOMETHING GREAT
© 2010 WILEY-VCH Verlag GmbH & Co. KGaA, Weinheim

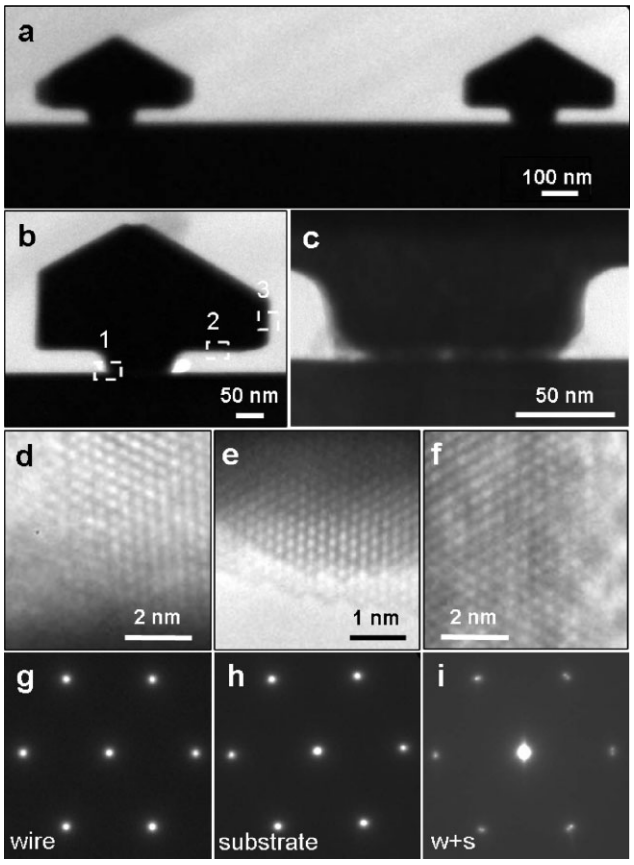

Figure 4. TEM cross-section view of the horizontal ZnO NWs with the substrate. a) Overview of two adjacent NWs. Enlarged view of b) a NW and c) the root area of the NW. HRTEM images of the areas d) 1, e) 2, and f) 3 in (b), as indicated by the white dashed boxes. Selected area electron diffraction patterns of g) the sole NW, h) the sole substrate, and i) the two together.

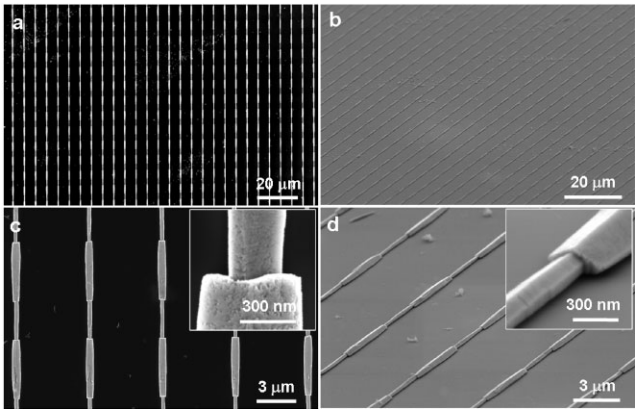

Figure 5. Horizontal ZnO NW-array-based two-segment monolithic superstructure. a) Top and b) 30° tilted view of the superstructure. Enlarged c) top and d) 30° tilted view of the thin and thick NWs connected together by lateral overgrowth. Inset images are an enlarged view of the connection junctions.

photoresist and each individual dot could be grown into a NW along the *c*-axis (Fig. S2).

Figure 4 depicts the cross section of the horizontal NWs by transmission electron microscopy (TEM). Photoresist on the substrate has been removed by baking at 500 °C for 30 min, which also helps improve the crystallinity of the NWs (see Fig. S3 for the surface morphology of the NWs before annealing). Just as we expected, the cross section of the NW appears like a "mushroom" with the root about 100-nm-wide, as defined by the size of the PO. The NW expands laterally, forming two wings after growing out of the PO. The separation between the wings and substrate surface is about 50 nm (Fig. 4b), which is the thickness of the photoresist. High-resolution TEM (HRTEM) images around the NW clearly indicate that on the $(2\bar{1}\bar{1}0)$ surface of the substrate, the as-grown NW is enclosed by well-defined $(01\bar{1}0)$ facets with a surface roughness of less than 2 nm (Fig. 4f). The electron-beam diffraction patterns from the sole NW (Fig. 4g) confirm its growth orientation along the *c*-axis, and those from the sole substrate (Fig. 4h) confirm the orientation of the substrate. The diffraction patterns of the two together, as shown in Figure 4i, clearly indicate their epitaxial orientation relationship.

We make use of the lateral overgrowth to make novel two-segment NW superstructures, as shown in Figure 5. To make the superstructures, we defined an array of POs with different widths separated from each other, for example, a row of 50-nm-wide POs, another row of 200-nm-wide POs, and so on. When the NWs grow out of the POs, they tend to expand and eventually merge or coalesce with each other (inset images show the junction regions), forming these continuous two-segment superstructures. By the same methodology, we can make multisegment NW superstructures, as shown in Figure 6, with the thinnest part only about 90-nm (inset of Fig. 6c) growing out of a 40-nm-wide PO (Fig. S4e). Each and every individual segment has an epitaxial relationship with the single-crystalline substrate, so the as-grown continuous superstructures are considered to be monolithic single crystals. Of course, the separation between the POs should be moderate to match the amount of lateral overgrowth the NWs could produce. The growth is very sensitive to the reaction temperature.[38] When the temperature is lowered from 85 to 80 °C, it changes from a well-faceted thick NW to a pile of thin NWs (Fig. S5). Using this methodology, we could fabricate an array of ultralong ZnO NWs with a length on the order of millimeters, width on the order of hundreds of nanometers, and aspect ratio on the order of ten thousand (Fig. S6). Compared with making an array of continuous ultralong POs, this also saves a lot of lithography exposure time. When fabricating these ultralong NWs, as discussed above, we also need to be careful about the orientation of the POs (Fig. S7).

The single-crystalline ZnO substrate is not only mechanically rigid and brittle, which prevents physical deformation from exerting on the NWs, but also electrically conductive, which obstructs us from fabricating electronic devices with the NWs on it. We demonstrate an effective way of lifting off these horizontal NWs and transferring them onto a mechanically flexible and electrically insulating polymer substrate (Fig. S8). First, we put a layer of methyl methacrylate (MMA) prepolymer on the as-grown superstructures. It is not necessary to remove the PMMA photoresist on the substrate simply because the prepolymer would form interfacial chemical bonds with the existing PMMA photoresist and give rise to a strong binding force between them. The viscosity of the prepolymer should be adequate so that it can

© 2010 WILEY-VCH Verlag GmbH & Co. KGaA, Weinheim

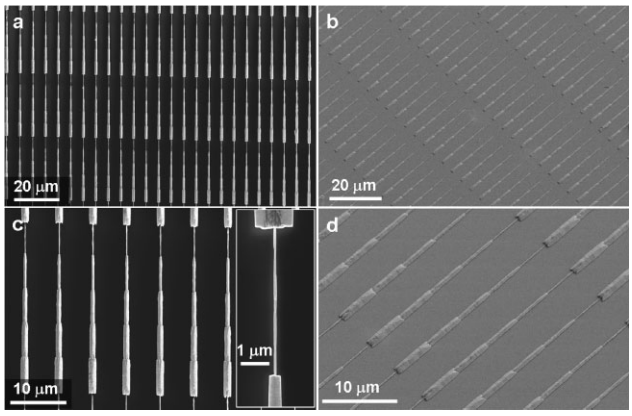

Figure 6. Horizontal ZnO NW-array-based five-segment monolithic superstructure. a) Top and b) 30° tilted view of the superstructure. Enlarged c) top and d) 30° tilted view of the five-segment superstructure. Inset image is an enlarged view of a thin NW at the connection junction.

form strong enough interface bonds, yet has sufficient fluidity to enclose all NWs without leaving any possible bubbles behind. After the prepolymer on the substrate was fully polymerized and about 100-μm thick, it was carefully lifted off the substrate together with the NWs, and thus the NWs were transferred onto the flexible PMMA substrate as shown in Figure 7b and c. Oxygen-plasma etching was used to etch a thin top surface layer of PMMA to partially expose the NWs. This could be easily scaled up to a large area, as shown in Figure 7d. Electrical transport properties of the as-transferred NW arrays were characterized by making connection leads at two ends of the arrays using In metal that forms an Ohmic contact. As shown in Figure 7e, the conductance of the arrays can be readily tuned by room light and UV light. Schottky contact is anticipated to have greater performance in this regard than Ohmic contact[7,30,31] and further study is still undergoing. Such a structure could have many important applications in flexible electronics and portable nanodevices.[39]

3. Conclusions

In summary, horizontally aligned ZnO NW arrays were rationally grown on the $(2\bar{1}\bar{1}0)$ surface of a single-crystalline ZnO substrate using a combination of a wet chemical method and electron-beam lithography. All of the NWs suffered from lateral overgrowth, but the width and length of the NWs could still be effectively controlled by defining different sizes of the POs. All of the NWs on the substrate grew strictly along the $\pm c$-axis no matter the orientations of the POs. A cross-sectional view of the NWs by TEM showed a ''mushroom-like'' structure and the NWs were enclosed by well-defined $(01\bar{1}0)$ facets and had a close epitaxial relationship with the substrate. We made use of the lateral overgrowth to fabricate novel monolithic multisegment superstructures by defining arrays of POs with different widths. Ultralong horizontal ZnO NW arrays with an aspect ratio on the order of ten thousand were also demonstrated by stepped lateral overgrowth. These superstructures were lifted off and transferred onto a flexible polymer substrate, which may have many potential applications in horizontal ZnO NW-based nanosensor arrays, light-emitting diodes, optical gratings, integrated circuit interconnects, and high-output-power alternating-current nanogenerators.

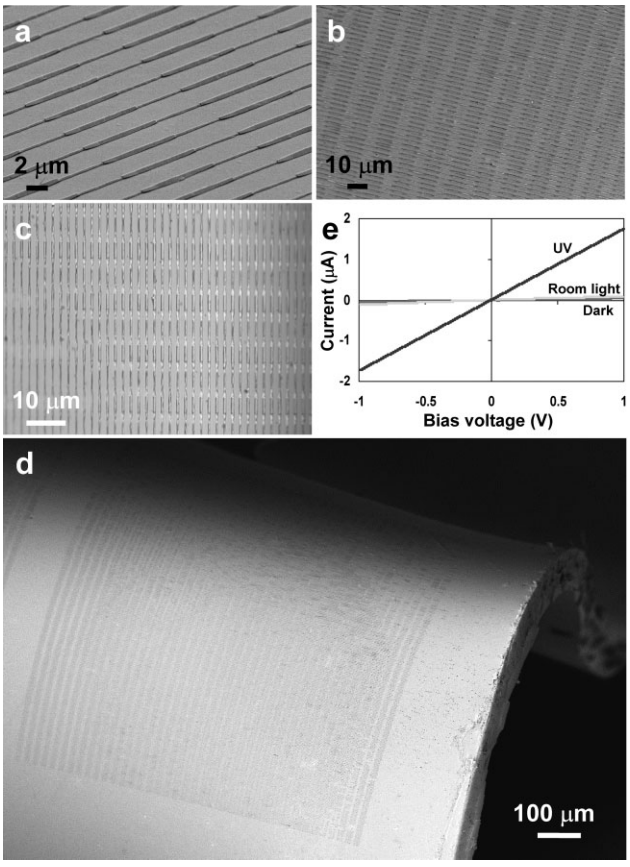

Figure 7. SEM images of the two-segment NW arrays a) on a ZnO substrate and b) after transferring on a flexible substrate. c) Bright-field optical image of the NW arrays on the flexible substrate. d) Low-magnification SEM image of the two-segment NW arrays on a flexible substrate. e) Current–voltage (I–V) curves of the as-transferred NW arrays in dark environment, under room light, and under UV illumination.

4. Experimental

The single-crystal ZnO $(2\bar{1}\bar{1}0)$ substrate with photoresist was prepared and post-treated by a standard process [29]. The patterns were defined by arrays of physical lines and rectangles with different lengths and widths, and also different orientations relative to the $\langle 0001 \rangle$ direction of the substrate. The line dose was ranged from 2.35 to 2.55 nC cm^{-1} for the physical lines and from 260 to 360 μC cm^{-2} for the rectangles. Hydrothermal growth was conducted by using a nutrient solution composed of a 1:1 ratio of zinc nitrate hexahydrate/hexamethylenetetramine for all the experiments, but with different concentrations. We floated the substrate facing down on the surface of the nutrient solution by virtue of surface tension of the aqueous solution [40]. The whole system was heated up to different temperatures (80 or 85 °C) for 2.5 h. After growth, it was cooled down to ambient temperature and then immersed in isopropyl alcohol (IPA) to remove the absorbed water.For the lift-off process, a thin layer of PMMA prepolymer was used, which was prepared by heating MMA monomer with 0.1% benzoyl peroxide at 95 °C for 15 min and then cooled down to room

WILEY InterScience DISCOVER SOMETHING GREAT
© 2010 WILEY-VCH Verlag GmbH & Co. KGaA, Weinheim

temperature. After that, the sample was kept at 50 °C for 10 h and 100 °C for 1 h to fully polymerize the prepolymer. Then the ZnO NWs were buried in the PMMA. After that the PMMA thin film was peeled away from the single-crystalline substrate and the horizontal NWs were transferred onto the PMMA thin film. Oxygen plasma was applied to the PMMA thin film to partially expose the buried NW arrays.

The as-grown and transferred horizontal ZnO NW arrays were characterized by scanning electron microscopy (SEM) at 5 kV and TEM at 400 kV using a JEM 4000EX.

Acknowledgements

Research was supported by DARPA (Army/AMCOM/REDSTONE AR, W31P4Q-08-1-0009), BES DOE (DE-FG02-07ER46394), KAUST, and NSF (DMS0706436, CMMI 0403671). Supporting Information is available online from Wiley InterScience or from the author.

Received: February 4, 2010
Published online: March 25, 2010

[1] Z. L. Wang, *Mater. Sci. Eng. R* **2009**, *64*, 33.
[2] M. H. Huang, S. Mao, H. Feick, H. Q. Yan, Y. Y. Wu, H. Kind, E. Weber, R. Russo, P. D. Yang, *Science* **2001**, *292*, 1897.
[3] G. C. Yi, W. I. Park, *Adv. Mater.* **2004**, *16*, 87.
[4] J. J. Cole, X. Wang, R. J. Knuesel, H. O. Jacobs, *Nano Lett.* **2008**, *8*, 1477.
[5] X. D. Bai, E. G. Wang, P. X. Gao, Z. L. Wang, *Nano Lett.* **2003**, *3*, 1147.
[6] M. Law, L. E. Greene, J. C. Johnson, R. Saykally, P. D. Yang, *Nat. Mater.* **2005**, *4*, 455.
[7] J. Zhou, Y. D. Gu, Y. F. Hu, W. J. Mai, P. H. Yeh, G. Bao, A. K. Sood, D. L. Polla, Z. L. Wang, *Appl. Phys. Lett.* **2009**, *94*, 191103.
[8] Z. L. Wang, J. H. Song, *Science* **2006**, *312*, 242.
[9] J. H. He, C. L. Hsin, J. Liu, L. J. Chen, Z. L. Wang, *Adv. Mater.* **2007**, *19*, 781.
[10] M. H. Huang, Y. Y. Wu, H. Feick, N. Tran, E. Weber, P. D. Yang, *Adv. Mater.* **2001**, *13*, 113.
[11] H. M. Cheng, H. C. Hsu, S. Yang, C. Y. Wu, Y. C. Lee, L. J. Lin, W. F. Hsieh, *Nanotechnology* **2005**, *16*, 2882.
[12] Y. Sun, G. M. Fuge, M. N. R. Ashfold, *Chem. Phys. Lett.* **2004**, *396*, 21.
[13] W. I. Park, D. H. Kim, S. W. Jung, G. C. Yi, *Appl. Phys. Lett.* **2002**, *80*, 4232.
[14] Y. W. Heo, V. Varadarajan, M. Kaufman, K. Kim, D. P. Norton, F. Ren, P. H. Fleming, *Appl. Phys. Lett.* **2002**, *81*, 3046.
[15] L. Vayssieres, *Adv. Mater.* **2003**, *15*, 464.
[16] J. J. Cole, X. Y. Wang, R. J. Knuesel, H. O. Jacobs, *Adv. Mater.* **2008**, *20*, 1474.
[17] S. H. Lee, I. H. Im, H. J. Lee, Z. Vashaei, T. Hanada, M. W. Cho, T. Yao, *Cryst. Growth Des.* **2006**, *6*, 2640.
[18] W. J. Mai, P. X. Gao, C. S. Lao, Z. L. Wang, A. K. Sood, D. L. Polla, M. B. Soprano, *Chem. Phys. Lett.* **2008**, *460*, 253.
[19] H. J. Fan, F. Fleischer, W. Lee, K. Nielsch, R. Scholz, M. Zacharias, U. Gosele, A. Dadgar, A. Krost, *Superlattices Microstruct.* **2004**, *36*, 95.
[20] J. H. Kim, D. Andeen, F. F. Lange, *Adv. Mater.* **2006**, *18*, 2453.
[21] T. F. Chung, L. B. Luo, Z. B. He, Y. H. Leung, I. Shafiq, Z. Q. Yao, S. T. Lee, *Appl. Phys. Lett.* **2007**, *91*, 233112.
[22] X. D. Wang, C. J. Summers, Z. L. Wang, *Nano Lett.* **2004**, *4*, 423.
[23] S. J. Kwon, P. Jae-Hwan, P. Jae-Gwan, *Appl. Phys. Lett.* **2005**, *87*, 133112.
[24] S. Xu, Y. Wei, M. Kirkham, J. Liu, W. Mai, D. Davidovic, R. L. Snyder, Z. L. Wang, *J. Am. Chem. Soc.* **2008**, *130*, 14958.
[25] Y. Qin, R. S. Yang, Z. L. Wang, *J. Phys. Chem. C* **2008**, *112*, 18734.
[26] J. I. Hong, J. Bae, Z. L. Wang, R. L. Snyder, *Nanotechnology* **2009**, *20*, 085609.
[27] N. Babak, A. M. Chris, J. S. Stephan, D. V. Mark, *Appl. Phys. Lett.* **2004**, *85*, 3244.
[28] O. Harnack, C. Pacholski, H. Weller, A. Yasuda, J. M. Wessels, *Nano Lett.* **2003**, *3*, 1097.
[29] S. Xu, Y. Ding, Y. G. Wei, H. Fang, Y. Shen, A. K. Sood, D. L. Polla, Z. L. Wang, *J. Am. Chem. Soc.* **2009**, *131*, 6670.
[30] P. H. Yeh, Z. Li, Z. L. Wang, *Adv. Mater.* **2009**, *21*, 4975.
[31] T. Y. Wei, P. H. Yeh, S. Y. Lu, Z. L. Wang, *J. Am. Chem. Soc.* **2009**, *131*, 17690.
[32] J. M. Bao, M. A. Zimmler, F. Capasso, X. W. Wang, Z. F. Ren, *Nano Lett.* **2006**, *6*, 1719.
[33] Z. W. Pan, S. M. Mahurin, S. Dai, D. H. Lowndes, *Nano Lett.* **2005**, *5*, 723.
[34] R. S. Yang, Y. Qin, L. M. Dai, Z. L. Wang, *Nat. Nanotechnol.* **2009**, *4*, 34.
[35] X. Y. Kong, Y. Ding, R. Yang, Z. L. Wang, *Science* **2004**, *303*, 1348.
[36] M. Kirkham, X. D. Wang, Z. L. Wang, R. L. Snyder, *Nanotechnology* **2007**, *18*, 365304.
[37] D. Andeen, J. H. Kim, F. F. Lange, G. K. L. Goh, S. Tripathy, *Adv. Funct. Mater.* **2006**, *16*, 799.
[38] S. Xu, N. Adiga, S. Ba, T. Dasgupta, C. F. J. Wu, Z. L. Wang, *ACS Nano* **2009**, *3*, 1803.
[39] Q. B. Xu, R. M. Rioux, M. D. Dickey, G. M. Whitesides, *Acc. Chem. Res.* **2008**, *41*, 1566.
[40] S. Xu, C. Lao, B. Weintraub, Z. L. Wang, *J. Mater. Res.* **2008**, *23*, 2072.

© 2010 WILEY-VCH Verlag GmbH & Co. KGaA, Weinheim